ISSN 1946-7664. MCFNS 2026
Vol. 18, Issue 2, pp. 106–115
Mathematical and Computational Forestry & Natural-Resource Sciences

AVAILABLE ONLINE AT HTTP://MCFNS.COM

Submitted: Sep. 28, 2026
Accepted: Oct. 30, 2026
Published: Oct. 30, 2026
Last Correction: Nov. 1, 2026

ABCDE: A BIDIRECTIONAL COUPLING OF DIFFERENTIAL EQUATIONS

DATA-TRENDS DERIVATION OF DYNAMIC SITE EQUATIONS FROM GROWTH RATES AND SITE GRADIENTS

Chris J. Cieszewski
Quantfor Co., Watkinsville, GA, USA

Abstract. I introduce here "*A Bidirectional Coupling of Differential Equations*" (ABCDE), yet another method for deriving flexible base-age-invariant, variable-age site index equations with polymorphism and variable asymptotes. My earlier approaches, including GADA and UTADA, concentrate on theory for formulating and structuring equations using theories of algebraic constructs. The ABCDE approach focuses instead on modeling the data trends of growth rates and site gradients that the final model should comprise. Its theories concern the component trends in two directions of the data structure, rather than presumed forms of asymptotes or growth rates. Simple height trends over age at fixed sites and over site quality at fixed ages supply two partial definitions: the longitudinal growth rate $P = H_t$ and the cross-sectional site gradient $Q = H_s$. Coupling them through the common integration of $dH = P\,dt + Q\,ds$ defines one surface $H(t, s)$ exactly when $P_s = Q_t$ on a simply connected domain. Compatibility also transfers information between directions: the growth rate and the index-age normalization (base-age conditioning) determine the site gradient, and the site gradient with one reference age profile determines the growth rate. Unique site inversion then gives a self-referencing dynamic equation with exact base-age invariance and path invariance as in the other methods. As with the foundational GADA and UTADA papers, this note presents general principles; empirical applications and method comparisons on specific data sets will follow separately in the future.

Keywords: GADA; UTADA; ABCDE method; VASI; BAI; path invariance; dynamic equations; self-referencing models; site models; site index; growth rate; site gradient; polymorphism; variable asymptotes.

1 Introduction

Dynamic site equations describe dominant height growth as a function of a reference height observed at an arbitrary reference age. They support site productivity assessment and stand growth projections in forest management (Clutter et al. 1983). A base-age-invariant (BAI) equation (Bailey and Clutter 1974) defines the exact same height–age trajectory regardless of which point along that trajectory is chosen as the reference observation. Variable-age site index (VASI; Cieszewski and Wawrykowicz 2025) permits that reference height to be specified at any arbitrary stand age rather than solely at a fixed conventional base age. Polymorphism allows the shapes and inflection points of height curves to change with site quality, and variable asymptotes allow their limiting heights to differ across sites (Cieszewski 2002).

The *Generalized Algebraic Difference Approach* (GADA; Cieszewski 1994; Cieszewski and Bailey 2000; Cieszewski 2004; Cieszewski and Strub 2008) and the *Unified Theory of the Algebraic Differences Approaches* (UTADA; Cieszewski 2021) provide general deductive theories for deriving dynamic site equations through algebraic operations on integral functions of height growth. Specifically, GADA begins with an explicit longitudinal height–age base function and replaces multiple parameters with functions of an unobservable site variable (in the sense of Judge et al. 1985, p. 705), whereas UTADA begins with a direct cross-sectional yield–site equation and modifies its parameters by functions of stand age. Both approaches concentrate on formulating and structuring closed-form algebraic equations.

A Bidirectional Coupling of Differential Equations (ABCDE) is a new method that I introduce here, in this note. This method relies on a complementary data-trends approach that concentrates on identifying from empirical data trends what directional rate components the final equation should comprise. While grounded in

Copyright © 2026 Publisher of the *Mathematical and Computational Forestry & Natural-Resource Sciences*

differential calculus, its theory concerns the empirical and theoretical trends in the two orthogonal directions of the age–site data structure rather than presumed integral forms of site-dependent height growth models. A longitudinal analysis describes height change over time at a fixed site (along *iso-site curves*); its partial derivative with respect to age is the *growth rate*. A cross-sectional analysis describes height change across site quality at a fixed age (along *iso-age curves*); its partial derivative with respect to site is the *site gradient*. Each directional analysis begins by fitting simple curves within slices of the data and then follows how their coefficients vary along the other coordinate. Each direction thereby supplies a partial differential definition of the desired surface. The ABCDE approach couples those two partial definitions by common integration of their differential equations. Enforcing mixed-derivative compatibility transfers structural information between the two directions, identifies required interaction terms that single-direction inspection would miss, and tests whether the proposed longitudinal and cross-sectional trends can coexist on a single surface.

As in the foundational GADA and UTADA papers (Cieszewski and Bailey 2000; Cieszewski 2021), the emphasis here is on the general mathematical principles of the approach. The term *data-trends* describes where the component structure of an ABCDE equation comes from—namely, from longitudinal growth-rate trends and cross-sectional site-gradient trends; I do not analyze a specific empirical data set in this note. The principles are general, and a worked data set would draw attention to its own sampling particulars rather than to the methodology itself. Empirical applications to specific forest data sets, together with direct comparisons against GADA and UTADA derivations, will follow separately in the future.

Let t denote stand age, s a scalar site coordinate, and $H(t,s)$ expected dominant height. The dynamic site equation has the self-referencing form

$$\begin{aligned} y &= F(t,t_0,y_0),\\ y_0 &= H(t_0,s), \qquad y = H(t,s). \end{aligned} \tag{1}$$

The reference age t_0 can vary arbitrarily; the same underlying site coordinate s connects the reference height y_0 at age t_0 and the target height y at age t. The fixed index (base) age t_* introduced below labels sites on a standardized scale and is distinct from the arbitrary reference age t_0 used for a prediction.

Specifying one curve in each direction does not by itself determine a two-dimensional surface, because any age–site interaction that vanishes along those two reference curves can be added without altering either curve. I write the two directional partial derivatives and the total differential of the height surface as

$$P = H_t, \qquad Q = H_s, \qquad dH = P\,dt + Q\,ds. \tag{2}$$

Here $P(t,s)$ is the longitudinal growth rate along a fixed-site trajectory and $Q(t,s)$ is the cross-sectional site gradient at fixed age. When height and site index are measured in meters and age in years, the units of P and Q are meters per year ($\mathrm{m\,yr^{-1}}$) and meters per meter ($\mathrm{m\,m^{-1}}$, dimensionless), respectively. The worked examples in Section 5 are analytical constructions from specified directional trends, not fitted empirical results.

2 Common Integration and Self-Reference

2.1 Compatibility and normalization

Assume that $P(t,s)$ and $Q(t,s)$ are continuously differentiable on a simply connected open age–site domain $\Omega \subset \mathbb{R}^2$. They are the partial derivatives of a single smooth surface $H(t,s)$ on Ω if and only if

$$P_s(t,s) = Q_t(t,s). \tag{3}$$

Necessity follows immediately from Clairaut's theorem on the equality of mixed partial derivatives ($H_{ts} = H_{st}$). Sufficiency is the exact differential one-form result associated with Poincaré's lemma (Olver 1993): when Eq. (3) holds on a simply connected domain, the line integral of $P\,dt + Q\,ds$ is independent of the integration path and defines a unique surface $H(t,s)$ up to an additive constant.

For explicit coordinate formulas, I use an age interval and a site interval whose Cartesian product lies within Ω and contains the integration paths. Define the site coordinate s as expected height at the chosen index age t_*, so that the surface satisfies the exact base-age model conditioning (MC; Cieszewski and Strub 2018)

$$H(t_*,s) = s.$$

Differentiating with respect to s requires the boundary condition $Q(t_*,s) = 1$ throughout the site interval. Integrating in age from t_* to t then yields

$$\begin{aligned} H(t,s) &= s + \int_{t_*}^{t} P(\tau,s)\,d\tau,\\ Q(t,s) &= 1 + \int_{t_*}^{t} P_s(\tau,s)\,d\tau. \end{aligned} \tag{4}$$

Thus compatibility is constructive: once the longitudinal growth rate $P(t,s)$ and the index-age normalization $H(t_*,s) = s$ are chosen, the cross-sectional site gradient $Q(t,s)$ is completely determined by the second line of

Eq. (4). Any proposed cross-sectional trend must agree with that integral expression, or else the directional pair (P, Q) must be revised. Note that the normalization $H(t_*, s) = s$ is a structural boundary condition across sites at the index age t_*, not a mere vertical shift of a surface whose index-age cross section has a non-identity shape.

Information also travels constructively in the opposite direction. Choose a reference site s_r and a longitudinal reference profile $h_r(t) = H(t, s_r)$ satisfying $h_r(t_*) = s_r$. Given a cross-sectional site gradient $Q(t, s)$ satisfying $Q(t_*, s) = 1$, integrating across site from s_r to s yields

$$\begin{aligned} H(t, s) &= h_r(t) + \int_{s_r}^{s} Q(t, \sigma)\, d\sigma, \\ P(t, s) &= h_r'(t) + \int_{s_r}^{s} Q_t(t, \sigma)\, d\sigma. \end{aligned} \tag{5}$$

Differentiating the first line with respect to s and t recovers $Q(t, s)$ and $P(t, s)$, and evaluating at $t = t_*$ recovers $H(t_*, s) = s_r + (s - s_r) = s$. The single reference profile $h_r(t)$ is required because integrating $H_s = Q$ with respect to s alone leaves an undetermined additive function of age. When both directional fields (P, Q) have been specified from data sub-analyses, one sets $h_r'(t) = P(t, s_r)$ and requires Eq. (3).

2.2 From the surface to the dynamic equation

Proposition 1. *Suppose that the common surface $H(t, s)$ is strictly one-to-one in s on the chosen site interval at every admissible reference age t_0. Write its unique site inverse at age t_0 as $s = S(t_0, y_0)$ for reference heights y_0 in that cross section's range. Then the transition function*

$$F(t, t_0, y_0) = H\big(t,\, S(t_0, y_0)\big) \tag{6}$$

is self-referencing and base-age invariant for all transitions within the admissible domain.

Proof. By definition of the inverse $S(t_0, y_0)$ at age t_0, $H(t_0, S(t_0, y_0)) = y_0$, so $F(t_0, t_0, y_0) = y_0$ (the self-referencing identity property). For any intermediate age t_1 and target age t_2, set $s_0 = S(t_0, y_0)$ and $y_1 = F(t_1, t_0, y_0) = H(t_1, s_0)$. Strict injectivity of $H(t_1, \cdot)$ on the site interval implies $S(t_1, y_1) = s_0$. Consequently,

$$\begin{aligned} F\big(t_2, t_1, F(t_1, t_0, y_0)\big) &= H\big(t_2, S(t_1, y_1)\big) = H(t_2, s_0) \\ &= F(t_2, t_0, y_0). \end{aligned} \tag{7}$$

This transitive composition property establishes path invariance and base-age invariance (PI and $\mathrm{BAI}_{\mathrm{pred}}$; Bailey and Clutter 1974; Cieszewski and Strub 2018). Setting $t_2 = t_0$ also guarantees exact reversibility back to the original reference point (t_0, y_0). □

By the inverse function theorem, $H(t_0, s)$ is locally invertible in s wherever $Q(t_0, s) = H_s(t_0, s) \neq 0$. The stronger monotonicity condition $Q(t, s) > 0$ throughout the site interval ensures global uniqueness of $S(t_0, y_0)$ at each age t_0, while existence requires that y_0 lie within the range of $H(t_0, \cdot)$ on the supported site interval. Compatibility ($P_s = Q_t$) alone does not supply positivity of Q: an isolated point where $Q = 0$ need not destroy strict monotonicity, but a sign change in Q indicates a fold (curve crossing across sites) and requires restricting the admissible domain.

Note that two distinct invariances operate in tandem: exactness ($P_s = Q_t$) makes the surface $H(t, s)$ independent of the integration path in the (t, s) plane, whereas unique site inversion in Eq. (7) makes height predictions $F(t, t_0, y_0)$ independent of the sequence of reference ages. Crucially, Proposition 1 holds whether $S(t_0, y_0)$ is obtained via a closed-form algebraic root or via bracketed numerical root-finding.

3 Directional Sub-Analyses of Data

In practice, stem analyses and remeasured permanent sample plots (PSPs) supply longitudinal height–age series, whereas the columns of a yield table provide smoothed longitudinal curves for discrete site classes. Conversely, temporary or permanent plots observed at common ages can supply cross-sectional height–site slices if a defensible site coordinate is available, and the rows of a yield table provide cross-sectional heights across site classes at fixed ages. Because site quality is an unobservable variable (Judge et al. 1985, p. 705), a temporary plot with a single height–age observation cannot independently identify its own true height at the index age t_*; site labels used in exploratory cross-sectional sub-analyses must therefore come from observed trajectories passing through t_*, auxiliary site information, or an explicitly stated preliminary estimation procedure.

To use directional sub-analyses as a structural discovery tool for formulating an ABCDE model, I propose the following eight-step sequence (where both directions must share the same dominant-height definition, target population, site scale $s = H(t_*, s)$, and supported age–site domain):

1. **Longitudinal slice regressions:** Fit parsimonious height–age functions within individual site classes or trajectories. Compare candidate curve families over the observed age range, retain parameter uncertainty, and identify which longitudinal coefficients govern scale, relative rate, and shape before tracking how they vary with site s.
2. **Cross-sectional slice regressions:** Fit parsimonious height–site functions across site classes at fixed

ages. Repeat these cross-sectional fits using several candidate index ages t_* (retaining series observed at both ages) to verify that the apparent cross-sectional functional form is not an artifact of a single reference age.

3. **Secondary coefficient trends:** Examine how the fitted longitudinal parameters vary across site s, and how the fitted cross-sectional parameters vary across age t. Fit simple parametric expressions to those coefficient progressions to identify the candidate terms required in the two-dimensional surface.
4. **Directional derivative fields:** Express both empirical descriptions in the common coordinate system (t, s), differentiate the longitudinal expression with respect to t to obtain $P(t, s)$ and the cross-sectional expression with respect to s to obtain $Q(t, s)$, and verify the index-age conditioning boundary $Q(t_*, s) = 1$.
5. **Integrability discrepancy diagnostic:** Compute the Integrability Discrepancy Index (IDI),

$$\mathrm{IDI}(t, s) = P_s(t, s) - Q_t(t, s), \tag{8}$$

which has units of yr^{-1} under the normalized coordinates and should be assessed within the common support of both directional descriptions. Mapping $\mathrm{IDI}(t, s)$ shows the location and sign of disagreement between P_s and Q_t; by itself, it is not a statistical test of the observations or evidence of a biological inconsistency, and it should be interpreted alongside the reconciliation and simultaneous estimation rules in Step 6 and the empirical residual diagnostics in Step 8.
6. **Reconciliation of directional fields:** If $\mathrm{IDI}(t, s) \neq 0$, state an explicit reconciliation rule. One rule is to treat the better-supported longitudinal rate $P(t, s)$ as primary and derive $Q(t, s)$ from Eq. (4); another is to treat the cross-sectional gradient $Q(t, s)$ and a reference profile $h_r(t)$ as primary via Eq. (5), compare the route surfaces in Eq. (9), or fit a compatible pair jointly. Any joint fit must declare the relative weights given to the two directional sources, and any resulting or combined surface must be re-differentiated to define its own compatible pair (P, Q) and confirm exactness $(P_s = Q_t)$.
7. **Common integration and site inversion:** Integrate the compatible pair (P, Q) to obtain the surface $H(t, s)$ normalized so $H(t_*, s) = s$, verify strict site monotonicity $Q(t, s) > 0$ over the intended domain, and invert $H(t_0, s) = y_0$ for $s = S(t_0, y_0)$ (algebraically or by bracketed root-finding) to form $F(t, t_0, y_0)$ in Eq. (6).
8. **Path and empirical validation:** Verify exact numerical identity and multi-step composition (Eq. 7) across forward and backward age transitions, and evaluate predictive residuals on independent or withheld longitudinal growth series.

Comparing the two canonical integration paths makes the role of $\mathrm{IDI}(t, s)$ concrete. Starting from (t_*, s_r) with height $H(t_*, s_r) = s_r$ and $Q(t_*, s) = 1$, integrating along s first and then t gives $H_L(t, s)$, whereas integrating along t first and then s gives $H_C(t, s)$:

$$\begin{aligned} H_L(t, s) &= s + \int_{t_*}^{t} P(\tau, s)\, d\tau, \\ H_C(t, s) &= s_r + \int_{t_*}^{t} P(\tau, s_r)\, d\tau + \int_{s_r}^{s} Q(t, \sigma)\, d\sigma. \end{aligned} \tag{9}$$

By Green's theorem (or the fundamental theorem of calculus), the path discrepancy between the two surfaces is the double integral of IDI over the rectangle $[t_*, t] \times [s_r, s]$:

$$H_L(t, s) - H_C(t, s) = \int_{t_*}^{t} \int_{s_r}^{s} \mathrm{IDI}(\tau, \sigma)\, d\sigma\, d\tau. \tag{10}$$

Compatible fields ($\mathrm{IDI} \equiv 0$) yield identical surfaces by both integration routes everywhere. Note that agreement of H_L and H_C at a single endpoint is insufficient because positive and negative values of IDI can cancel in Eq. (10); likewise, if $H_L \neq H_C$, simply averaging the two incompatible surfaces alters both partial derivatives and requires reporting the modified directional rates.

Finally, because cross-sectional inventory data can confound stand age and site quality through historical harvesting patterns, cohort differences, or silvicultural selection—and because traditional yield tables represent smoothed group averages rather than raw stochastic trajectories—the directional sub-analyses in Steps 1–5 serve to discover the *structural algebraic form* of the compatible surface $H(t, s)$, after which final parameter calibration on noisy observations should use simultaneous base-age-invariant fixed-effects estimation (Cieszewski and Bailey 2000; Cieszewski and Strub 2018).

4 What Directional Trends Imply

4.1 Proportional and site-linear sections

When cross-sectional iso-age slices are strictly proportional to site index s under the normalization at t_*, the surface and its partial derivatives take the separable ratio form

$$\begin{aligned} H(t, s) &= s\, \frac{g(t)}{g(t_*)}, \\ P(t, s) &= s\, \frac{g'(t)}{g(t_*)}, \qquad Q(t, s) = \frac{g(t)}{g(t_*)}, \end{aligned} \tag{11}$$

with $g(t) > 0$ on the age domain. Here $P_s = Q_t = g'(t)/g(t_*)$ and the relative height ratio $H(t, s)/s =$

$g(t)/g(t_*)$ is independent of s. All longitudinal trajectories have identical proportional shapes, which is the classical *anamorphic* case (Clutter et al. 1983; Cieszewski 2021). Conversely, any family of positive anamorphic trajectories normalized by index-age height has the form of Eq. (11).

Allowing the linear cross-sectional iso-age slices to have an age-dependent intercept $\alpha(t)$ in addition to a slope $\beta(t)$ yields the affine site-linear surface

$$\begin{aligned} H(t,s) &= \alpha(t) + \beta(t)s, \\ P(t,s) &= \alpha'(t) + \beta'(t)s, \qquad Q(t,s) = \beta(t), \\ \alpha(t_*) &= 0, \qquad \beta(t_*) = 1. \end{aligned} \tag{12}$$

Compatibility holds identically since $P_s = \beta'(t) = Q_t$. Conversely, specifying a longitudinal growth rate linear in site, $P(t,s) = p_0(t) + p_1(t)s$, together with $H(t_*, s) = s$ produces Eq. (12) via

$$\alpha(t) = \int_{t_*}^{t} p_0(\tau)\, d\tau, \qquad \beta(t) = 1 + \int_{t_*}^{t} p_1(\tau)\, d\tau. \tag{13}$$

Whenever $\alpha(t) \neq 0$ at some age $t \neq t_*$, the normalized ratio $H(t,s)/s = \alpha(t)/s + \beta(t)$ varies with s and the longitudinal trajectories are *polymorphic* (reducing to the anamorphic case Eq. 11 only when $\alpha(t) \equiv 0$). If finite limits $\alpha_\infty = \lim_{t\to\infty} \alpha(t)$ and $\beta_\infty = \lim_{t\to\infty} \beta(t)$ exist, the limiting height is $M(s) = \alpha_\infty + \beta_\infty s$, which yields variable asymptotes whenever $\beta_\infty \neq 0$ and a single common asymptote α_∞ if $\beta_\infty = 0$. In site-linear or higher-order rational/power formulations, finite positive asymptotes require the appropriate limiting behavior of the age functions as $t \to \infty$.

4.2 Asymptotes and site-dependent rate coefficients

More generally, for any normalized longitudinal growth rate $P(t,s)$ whose improper integral converges as $t \to \infty$, the limiting asymptotic height is

$$M(s) = \lim_{t\to\infty} H(t,s) = s + \int_{t_*}^{\infty} P(\tau, s)\, d\tau. \tag{14}$$

The model possesses variable asymptotes (Cieszewski 2002) precisely when $M(s)$ is nonconstant; where the limit and the site derivative can be interchanged, $M'(s) = \lim_{t\to\infty} Q(t,s)$. Whether $M(s)$ varies with s is distinct from whether the curves are anamorphic or polymorphic, and finite-age inventory data alone do not guarantee that an extrapolated mathematical asymptote $M(s)$ represents a physiological ceiling.

When a longitudinal rate coefficient $k(s)$ varies with site quality s (as in exponential or Richards GADA models; Cieszewski 2004; Cieszewski and Strub 2008), it rescales the biological clock of stand development across sites. As demonstrated in Example 2 below, differentiating an exponential growth rate with respect to its site-dependent rate parameter $k(s)$ generates a mandatory secular interaction term in the site gradient $Q(t,s)$. Table 1 summarizes these structural implications.

5 Constructed Examples

5.1 Example 1: separable rates and quadratic site scaling

Let $u = t - t_* \geq 0$ and $s > 0$. Suppose the longitudinal sub-analysis indicates an exponential decline in height increment with a quadratic site amplitude, while the cross-sectional sub-analysis indicates a site gradient linear in s with an age-dependent multiplier. Write the independently proposed directional fields as

$$\begin{aligned} P(t,s) &= ke^{-ku}\big(as + bs^2\big), \\ Q(t,s) &= 1 + \big(1 - e^{-ku}\big)(c + 2ds), \end{aligned} \tag{15}$$

where $k, a, b > 0$ and c, d are initially separate cross-sectional coefficients. Their mixed partial derivatives are

$$\begin{aligned} P_s(t,s) &= ke^{-ku}(a + 2bs), \\ Q_t(t,s) &= ke^{-ku}(c + 2ds). \end{aligned} \tag{16}$$

Enforcing $P_s = Q_t$ over a nontrivial site interval immediately forces $c = a$ and $d = b$. Common integration via Eq. (4) with $H(t_*, s) = s$ yields the compatible surface

$$H(t,s) = s + \big(1 - e^{-ku}\big)\big(as + bs^2\big). \tag{17}$$

Integrating Q with respect to s via Eq. (5) gives the identical surface once the age-only integration function is matched to $H_t = P$ and $H(t_*, s) = s$. For $k, a, b > 0$ and $u \geq 0$, we have $P(t,s) > 0$, $Q(t,s) = 1 + (1 - e^{-ku})(a + 2bs) \geq 1$, and a site-varying asymptote $M(s) = (1 + a)s + bs^2$. Remarkably, even though $P(t,s)$ in Eq. (15) is multiplicatively separable in u and s, the normalized height ratio $H(t,s)/s = 1 + (1 - e^{-ku})(a + bs)$ depends on s for all $u > 0$, so the longitudinal curves are polymorphic whenever $b > 0$.

For any reference age $t_0 \geq t_*$, define $D_0 = 1 - e^{-k(t_0 - t_*)}$ and $C_0 = 1 + aD_0$. Inverting $H(t_0, s) = y_0$ yields the quadratic site equation $bD_0 s^2 + C_0 s - y_0 = 0$, whose unique positive root in rationalized (Citardauq) form is

$$S(t_0, y_0) = \frac{2y_0}{C_0 + \sqrt{C_0^2 + 4bD_0 y_0}}. \tag{18}$$

For $y_0 > 0$ the denominator is strictly positive, and as $t_0 \to t_*$ ($D_0 \to 0$, $C_0 \to 1$) Eq. (18) reduces smoothly

Table 1: Directional trends and the model properties they imply under the index-age normalization $H(t_*, s) = s$.

Directional pattern	Compatible surface or required term	Structural implication
Proportional height–site sections	$H(t,s) = s\,g(t)/g(t_*)$; Eq. (11)	Strictly anamorphic trajectories; linear iso-age lines through the origin.
Site-linear sections with age-dependent intercept and slope	$H(t,s) = \alpha(t) + \beta(t)s$; equivalently, normalized $P(t,s)$ is linear in s; Eqs. (12)–(13)	Polymorphic if $\alpha(t) \not\equiv 0$; variable asymptotes if finite limits exist and $\beta_\infty \neq 0$.
Longitudinal limiting height depends on site	$M(s) = s + \int_{t_*}^{\infty} P(\tau, s)\, d\tau$ is nonconstant; Eq. (14)	Variable asymptotes; curve-shape polymorphism remains a separate property.
Site-dependent exponential rate $k(s) = k_0 + k_1 s$, $k_1 > 0$ (Example 2)	$Q(t,s)$ must contain the secular interaction term $+Ak_1 s(t - t_*)e^{-k(s)(t-t_*)}$; Eq. (23)	Polymorphism driven by a site-dependent time scale; mandatory transient interaction in Q.

to $S(t_*, y_0) = y_0$ without division by zero. Substituting $S = S(t_0, y_0)$ into Eq. (17) gives the closed-form dynamic equation

$$F(t, t_0, y_0) = S + \big(1 - e^{-k(t-t_*)}\big)\big(aS + bS^2\big), \quad S = S(t_0, y_0). \tag{19}$$

5.2 Example 2: a site-dependent rate constant

Now let the relative rate parameter increase linearly with site quality, $k(s) = k_0 + k_1 s$, with $A, k_0, k_1 > 0$, $s > 0$, and $u = t - t_* \geq 0$. A longitudinal sub-analysis with a site-dependent exponential rate suggests

$$P(t, s) = As\,k(s)\,e^{-k(s)u}. \tag{20}$$

To determine what cross-sectional structure its counterpart $Q(t, s)$ requires, consider the candidate family

$$Q(t, s) = 1 + B\big(1 - e^{-k(s)u}\big) + Csue^{-k(s)u}, \tag{21}$$

where B and C are initially free coefficients. Writing $k = k(s)$ for brevity, the mixed derivatives are

$$\begin{aligned} P_s(t, s) &= A\big[k + k_1 s - k_1 sku\big]e^{-ku}, \\ Q_t(t, s) &= \big[Bk + Cs - Csku\big]e^{-ku}. \end{aligned} \tag{22}$$

Matching the coefficients of the secular term ue^{-ku} forces $C = Ak_1$, and matching the remaining terms forces $B = A$. Consequently, the unique compatible cross-sectional site gradient is

$$Q(t, s) = 1 + A\big(1 - e^{-ku}\big) + Ak_1 sue^{-ku}. \tag{23}$$

The final term $+Ak_1 sue^{-ku}$ is a mandatory secular interaction term generated by differentiating $\exp(-k(s)u)$ with respect to its site-dependent rate $k(s)$. It vanishes at $u = 0$ and decays to zero as $u \to \infty$, but omitting it at intermediate ages would render Q mathematically incompatible with P.

Common integration via Eq. (4) gives the surface

$$H(t, s) = s + As\big(1 - e^{-(k_0 + k_1 s)(t - t_*)}\big), \tag{24}$$

with variable asymptote $M(s) = (1 + A)s$ and polymorphic relative trajectory $H(t, s)/s = 1 + A(1 - e^{-k(s)u})$. To invert Eq. (24) at $t_0 \geq t_*$ ($u_0 = t_0 - t_* \geq 0$), we solve

$$R(s) = s + As\big(1 - e^{-(k_0 + k_1 s)u_0}\big) - y_0 = 0. \tag{25}$$

Because its derivative with respect to s satisfies

$$\begin{aligned} R'(s) &= H_s(t_0, s) \\ &= 1 + A\big(1 - e^{-ku_0}\big) + Ak_1 su_0 e^{-ku_0} \geq 1, \end{aligned} \tag{26}$$

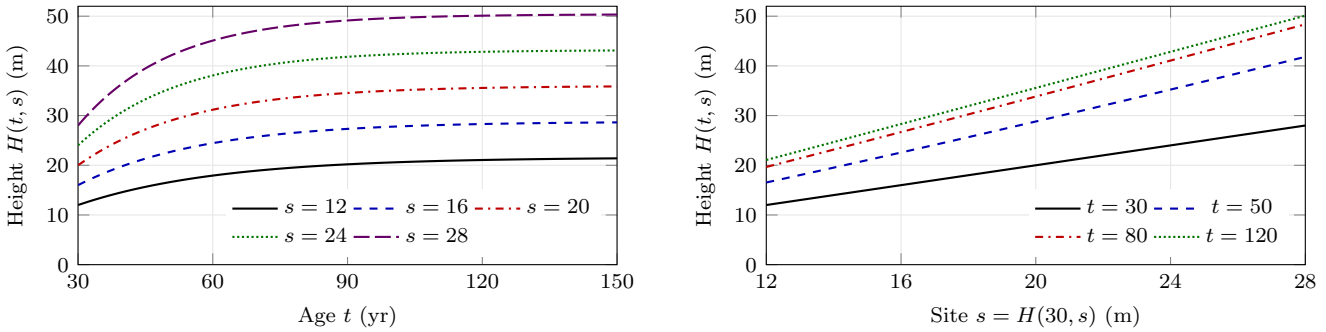
the root $S(t_0, y_0)$ is globally unique for every $y_0 > 0$. Moreover, since $s \leq H(t_0, s) \leq (1 + A)s$ for $u_0 \geq 0$, $S(t_0, y_0)$ always lies inside the closed bracket

$$\frac{y_0}{1 + A} \leq S(t_0, y_0) \leq y_0, \tag{27}$$

where $R(y_0/(1 + A)) \leq 0$ and $R(y_0) \geq 0$. For $u_0 < 0$, both endpoint residuals are negative and $H(t_0, s) < s$ for $s > 0$; any positive root, if one exists, satisfies $S > y_0$. Extension below the index age requires a separately verified monotone site domain, admissible reference-height range, and sign-changing root bracket. On the stated $u_0 \geq 0$ domain, bisection or Brent's bracketed method recovers $S(t_0, y_0)$ to machine precision, yielding the dynamic equation

$$F(t, t_0, y_0) = S + AS\big(1 - e^{-k(S)(t-t_*)}\big), \quad S = S(t_0, y_0). \tag{28}$$

Figure 1 illustrates the longitudinal iso-site curves and cross-sectional iso-age curves of Eq. (24).



(a) Longitudinal sections; site s in meters.

(b) Cross sections; age t in years.

Figure 1: Two directions of the Example 2 surface, Eq. (24), with $t_* = 30$ yr, $A = 0.80$, $k_0 = 0.02$ yr^{-1}, and $k_1 = 0.001$ m^{-1}yr^{-1}: (a) longitudinal sections at fixed site s and (b) cross sections at fixed age t (where $t = 30$ is the index-age conditioning line $H(30, s) = s$ with $Q = 1$). Every curve is drawn from the same formula.

5.3 Example 3: the site-linear dynamic equation

For the affine site-linear surface in Eq. (12) with $\beta(t) > 0$, direct algebraic inversion for $S(t_0, y_0)$ and substitution into $H(t, S)$ yield

$$\begin{aligned} S(t_0, y_0) &= \frac{y_0 - \alpha(t_0)}{\beta(t_0)}, \\ F(t, t_0, y_0) &= \alpha(t) + \frac{\beta(t)}{\beta(t_0)}\big[y_0 - \alpha(t_0)\big]. \end{aligned} \tag{29}$$

At $t = t_0$, $F(t_0, t_0, y_0) = y_0$, and multi-step composition via any intermediate age t_1 cancels $\alpha(t_1)$ and $\beta(t_1)$ identically, reducing to the anamorphic equation $F(t, t_0, y_0) = y_0\beta(t)/\beta(t_0)$ when $\alpha(t) \equiv 0$. Choosing α and β with $\alpha(0) = \beta(0) = 0$ in addition to $\alpha(t_*) = 0$, $\beta(t_*) = 1$ also enforces $H(0, s) = 0$ at stand origin.

5.4 Numerical composition checks

For Example 1, take $t_* = 30$ yr, $k = 0.04$ yr^{-1}, $a = c = 0.25$, $b = d = 0.015$ m^{-1}, and $s = 20$ m, giving an asymptote of $M(20) = 31$ m. For Example 2, take $t_* = 30$ yr, $A = 0.80$, $k_0 = 0.02$ yr^{-1}, $k_1 = 0.001$ m^{-1}yr^{-1}, and $s = 20$ m, so that $k(20) = 0.04$ yr^{-1} and $M(20) = 36$ m; Eq. (26) also confirms that $\min Q(t, s) = 1.0$ over $30 \le t \le 200$ yr and $5 \le s \le 40$ m (attained at $t = t_*$). Table 2 reports the direct and multi-step composed predictions using the Citardauq root (Eq. 18) for Example 1 and bracketed Brent root-finding (Eqs. 25–27) for Example 2, confirming Proposition 1 to six decimal places.

6 Scope and Limitations

Although the ABCDE method systematically identifies and couples directional rate components, every construction requires five operational checks:

1. *Compatibility.* If $P_s \neq Q_t$ anywhere in the domain, no smooth surface possesses both proposed derivative fields; integration cannot remove that discrepancy without imposing parameter constraints, choosing a primary direction, or performing a joint compatible fit.
2. *Integration.* Compatible continuous fields (P, Q) on a simply connected domain define a unique surface even when the integrals in Eqs. (4)–(5) require numerical quadrature. In Examples 1 and 2, restricting $t \ge t_*$ permits forward projection and backward projection toward t_*; extending predictions to juvenile ages $0 < t < t_*$ requires verifying $H(t, s) > 0$ and $Q(t, s) > 0$ throughout the intended age–site domain.
3. *Inversion.* The supported site interval must admit a unique root $S(t_0, y_0)$ at each reference age t_0. At fixed t_0 where $Q(t_0, S) \neq 0$, differentiating $H(t_0, S(t_0, y_0)) = y_0$ gives $Q(t_0, S)\,\partial S/\partial y_0 = 1$, hence $\partial S/\partial y_0 = 1/Q(t_0, S)$. Thus a small $|Q|$ amplifies small height measurement errors in the inferred site quality to first order, even where an inverse exists.
4. *Biological and statistical validity.* Neither mixed-derivative compatibility nor base-age invariance establishes empirical accuracy; final parameter estimation on longitudinal observations must account for measurement and process errors in reference heights, serial autocorrelation within growth series, and extrapolation uncertainty.
5. *Site dimension.* This note assumes a scalar site coordinate s. With $m > 1$ independent site coordinates $\mathbf{s} = (s_1, \ldots, s_m)$ and gradients $Q_i = H_{s_i}$, integrability of $dH = P\,dt + \sum_i Q_i\,ds_i$ requires $P_{s_i} = (Q_i)_t$ and $(Q_i)_{s_j} = (Q_j)_{s_i}$, and identifying all m site coordinates for a stand requires multiple observations or auxiliary biophysical covariates.

Table 2: Direct and composed height predictions for Examples 1 and 2. Heights are in meters.

Example	Target age (yr)	$F(t, 30, 20)$	Alternate reference path	Result
1	30	20.000000	$F(30, 30, 20)$	20.000000
1	40	23.626479	—	—
1	60	27.686864	$F(60, 40, F(40, 30, 20))$	27.686864
1	80	29.511312	$F(80, 60, F(60, 30, 20))$	29.511312
2	40	25.274879	—	—
2	60	31.180893	$F(60, 40, F(40, 30, 20))$	31.180893
2	80	33.834635	$F(80, 60, F(60, 30, 20))$	33.834635
2	30	20.000000	$F(30, 80, F(80, 30, 20))$	20.000000

The direct values also equal $H(t, 20)$. Intermediate predictions are carried at full floating-point precision without rounding; displayed results are rounded to six decimals.

7 Discussion

Dominant height growth models are used for site productivity classification, stand yield projections, and the planning of silvicultural treatments and harvests (Clutter et al. 1983). In timber supply modeling, inaccurate height predictions propagate through volume equations and can influence rotation timing and allowable annual cut (AAC) determinations; the direction and magnitude of those effects depend on the entire growth-and-yield systems that are built from individual equations. Because managed forests rarely have their dominant height measured at a fixed base age, forest managers must rely on inventory measurements taken at whatever age a stand has reached. Self-referencing VASI equations use such a measurement directly to predict the stand's height at any other age (Cieszewski and Strub 2018; Cieszewski and Wawrykowicz 2025). Like the GADA and UTADA equations, the dynamic site equations derived with ABCDE are base-age invariant and path invariant.

Well-behaved site models must also be flexible enough to describe complex data trends. Where site quality affects both the timing of growth and the final height, a model restricted to anamorphic curves (the same shape on all sites) or to a single common asymptote is likely to be biased on some sites. Yet it is not sufficient to derive just any equation that is polymorphic and has variable asymptotes; the specific patterns of polymorphism and of change in the asymptotes must agree with biological reality and with the data on hand (Cieszewski 2002). ABCDE takes these patterns from the growth and site trends in the data. Examples 1 and 2 have both properties, but whether such flexibility improves predictions, including AAC forecasts, must be shown by fitting and testing the models on representative data.

Site models have evolved from simple anamorphic, through simple polymorphic, to complex polymorphic forms, and from static models based on fixed-base-age site index to dynamic equations (Cieszewski 2021). Static models can take complex shapes. With base-age-specific fitting, parameter estimates can change when the base age changes, and separately fitted height and site index equations are not exact inverses of each other. Successive inventory updates can then produce inconsistent growth curves (Bailey and Clutter 1974; Cieszewski 2002). Rose et al. (2003) showed examples of such erroneous inventory predictions with incompatible site index and height models for jack pine in Ontario. The algebraic difference approach (ADA; Bailey and Clutter 1974) produced base-age-invariant dynamic equations, but they were mostly either anamorphic with variable asymptotes or polymorphic with a common asymptote (Cieszewski and Bailey 2000; Cieszewski 2002). GADA (Cieszewski 1994; Cieszewski and Bailey 2000; Cieszewski 2004; Cieszewski and Strub 2008) and UTADA (Cieszewski 2021) removed this limitation by letting several parameters of a base equation change with site (GADA) or with age (UTADA).

Both GADA and UTADA begin with a selected equation for height itself and then modify its parameters. Because the parameters of nonlinear growth equations interact, it can be difficult to foresee how a given set of modifications will shape both the growth over age and the differences among sites. ABCDE begins from the other end. The modeler first examines two simple kinds of data trends: how height changes with age on a given site (the growth rate) and how height changes with site at a given age (the site gradient). The method then finds the single height–age–site surface that reconciles both. ABCDE complements GADA and UTADA rather than replacing them; different routes may lead to the same dynamic equation, and the contribution of ABCDE is to make the evidence from both directions, and the conditions needed to reconcile them, explicit.

Coupling the two directions does more than check whether the two trends can coexist. Each direction carries information about the other, so the coupling can reveal terms and links between parameters that an analysis of only one direction may miss. With trends fit-

ted to data, the Integrability Discrepancy Index (IDI; Section 3) shows where, and by how much, they disagree. Such disagreement points to unsuitable model forms, or to differences between the longitudinal and cross-sectional samples, rather than by itself to errors in the data.

Two practical requirements remain. First, estimating the site gradient requires a dependable site measure for each stand; a single height and age measurement from a temporary plot does not by itself establish the stand's height at the index age. Second, each height at a given age must belong to only one site, so that the curves of different sites never cross; this is what allows a dynamic equation to find the site of a stand from a single measurement. A site gradient that stays positive at all ages ensures this.

As with GADA (Cieszewski and Bailey 2000), I recommend ABCDE as a tool and not as an ideology. It does not pre-empt any statistical assumptions about error structures or fitting criteria.

8 Summary

In this note, I introduced *A Bidirectional Coupling of Differential Equations* (ABCDE) for the data-trends derivation of flexible BAI and VASI dynamic site equations with polymorphism and variable asymptotes, shifting the emphasis from the purely algebraic structuring of three-dimensional equations to the coupled longitudinal growth-rate ($P = H_t$) and cross-sectional site-gradient ($Q = H_s$) trends in the fitting data, which are simpler, two-dimensional relationships. Enforcing exact integrability ($P_s = Q_t$) transfers structural information between directions—identifying mandatory secular interaction terms when rate parameters vary with site—and index-age normalization with unique site inversion yields a self-referencing dynamic equation satisfying exact base-age invariance, path invariance, and model conditioning. As with the foundational GADA and UTADA papers, this note sets out general principles; empirical applications and comparisons on specific data sets will be reported separately.

9 Biographical Note

This note concludes a long personal journey in my search for flexible, self-referencing site models. When I began studying forestry in 1972, base-age invariance had not yet been formally established in forestry biometrics (Bailey and Clutter 1974). In 1982, when I first sought to use self-referencing height models in my academic work in Poland, *only* printed yield tables were available to me. The following year, after fleeing Poland and its communist security apparatus,[1] I moved to Canada, where I encountered *only* fixed-base-age site-index models. I was told that the VASI models then used in the southeastern United States were *only* anamorphic or simply polymorphic with a common asymptote, and that these formulations did not meet the modeling needs of researchers in Canada or the western United States.

At the University of British Columbia, I developed an advanced VASI model combining polymorphism with variable asymptotes (Cieszewski 1988; later published as Cieszewski and Bella 1989). To my knowledge, it was then the *only* VASI model with advanced polymorphism and variable asymptotes. I subsequently developed a general, tractable methodology for systematically deriving such equations. This framework formed part of my doctoral dissertation (Cieszewski 1994) and was later published as the generalized algebraic difference approach (GADA; Cieszewski and Bailey 2000)—at the time, the *only* published methodology for systematically deriving advanced polymorphic VASI equations with variable asymptotes.

9.1 From "*only*" to "*ilno*"

After several further advances, I can finally declare an end to "*only*" in this field. The state of the art now invites the opposite expression: "*ilno*." I introduce *ilno* as the antonym of *only* in the attitude it conveys toward a stated quantity. *Only* suggests disappointment that the amount is less than one might have expected or hoped for: it could have been more, but it is not. *Ilno* expresses the opposite reaction—surprise that the amount is that great. Neither word changes the stated value; each places the same fact in relation to a different expectation.

Consider two statements: "My body temperature is *ilno* 105 °F!" and "The oven temperature is *only* 105 °F." The same numerical temperature is unexpectedly and alarmingly high in the first context, yet disappointingly low in the second. The words do not change the measurement or assert that the number is intrinsically large or small. They convey opposite reactions to what that measurement means in context.

Polish expresses this contrast compactly through *tylko* ("only") and *aż* ("surprisingly that much," hence "ilno"). English can approximate the latter with "as many as," "as much as," or "a whopping," but lacks an equally concise, single-word counterpart to *only* conveying the same contrasting emphasis. Descriptions such as "huge" and "pitiful" judge the magnitude itself, whereas *ilno* and *only* convey its significance relative to expecta-

[1] The Polish *Służba Bezpieczeństwa* (SB) was the communist-era security service; the earlier *Urząd Bezpieczeństwa* (UB) was its predecessor. Both were closely connected with the Soviet KGB.

tion. I form *ilno* by reversing *only* to *ylno* and replacing the initial "y" with "i" for easier pronunciation. I have not found an established English use of the word in this sense, or any use of "ilno" at all.

Thus, where we once had *only* fixed-base-age models and then *only* one published general derivation methodology, we now have *ilno* several methodologies and an even greater number of powerful VASI models—a change from scarcity to an abundance of options.

9.2 In Closing

We now have *ilno* five published methodologies—the three methods of Cieszewski (2001), UTADA (Cieszewski 2021), and ABCDE—capable of deriving complex polymorphic VASI equations with variable asymptotes, and several further approaches are in the works. Flexible, self-referencing dynamic site models are therefore no longer a methodological rarity. The challenge has shifted from whether such models can be constructed to determining which structures are best supported by the available evidence—the question that ABCDE addresses through the joint analysis of growth-rate and site-gradient trends.

Acknowledgements

I thank Aaron Weiskittel, Mike Strub, and the anonymous reviewers for their helpful comments on the manuscript.

References

Bailey, R.L., and Clutter, J.L. 1974. Base-age invariant polymorphic site curves. *For. Sci.* 20(2): 155–159.

Cieszewski, C.J. 1988. New polymorphic height growth and site index model for lodgepole pine in Alberta. M.F. major paper, Univ. of British Columbia, Vancouver, BC.

Cieszewski, C.J. 1994. Development of a variable density height-growth-model through defining multidimensional height growth spaces. Ph.D. thesis, Univ. of Alberta, Edmonton, AB, 72 p.

Cieszewski, C.J. 2001. Three methods of deriving advanced dynamic site equations demonstrated on inland Douglas-fir site curves. *Can. J. For. Res.* 31(1): 165–173.

Cieszewski, C.J. 2002. Comparing fixed- and variable-base-age site equations having single versus multiple asymptotes. *For. Sci.* 48(1): 7–23.

Cieszewski, C.J. 2004. GADA derivation of dynamic site equations with polymorphism and variable asymptotes from Richards, Weibull, and other exponential functions. Univ. of Georgia PMRC-TR 2004-5, Athens, GA, 16 p.

Cieszewski, C.J. 2021. UTADA: Unified Theory of the Algebraic Differences Approaches—Derivation of dynamic site equations from direct yield-site relationships. *Math. Comput. For. Nat.-Res. Sci.* 13(1): 36–43.

Cieszewski, C.J., and Bailey, R.L. 2000. Generalized algebraic difference approach: theory based derivation of dynamic site equations with polymorphism and variable asymptotes. *For. Sci.* 46(1): 116–126.

Cieszewski, C.J., and Bella, I.E. 1989. Polymorphic height and site index curves for lodgepole pine in Alberta. *Can. J. For. Res.* 19(9): 1151–1160.

Cieszewski, C.J., and Strub, M. 2008. Generalized algebraic difference approach derivation of dynamic site equations with polymorphism and variable asymptotes from exponential and logarithmic functions. *For. Sci.* 54(3): 303–315.

Cieszewski, C.J., and Strub, M. 2018. Comparing properties of self-referencing models based on nonlinear-fixed-effects versus nonlinear-mixed-effects modeling approaches. *Math. Comput. For. Nat.-Res. Sci.* 10(2): 46–57.

Cieszewski, C.J., and Wawrykowicz, A.A. 2025. VASIP: Visualizing measurement and process errors in VASI equations based on Monserud's site index model. *Math. Comput. For. Nat.-Res. Sci.* 17(2): 41–57.

Clutter, J.L., Fortson, J.C., Pienaar, L.V., Brister, G.H., and Bailey, R.L. 1983. *Timber Management: A Quantitative Approach*. John Wiley & Sons, New York, NY, 333 p.

Judge, G.G., Griffiths, W.E., Hill, R.C., Lütkepohl, H., and Lee, T.C. 1985. *The Theory and Practice of Econometrics*, 2nd ed. John Wiley & Sons, New York, NY, 1019 p.

Olver, P.J. 1993. *Applications of Lie Groups to Differential Equations*, 2nd ed. Graduate Texts in Mathematics 107. Springer, New York, NY, 513 p.

Rose, C.E., Cieszewski, C.J., and Carmean, W.H. 2003. Three methods for avoiding the impacts of incompatible site index and height prediction models demonstrated on jack pine curves for Ontario. *For. Chron.* 79(5): 928–935.